Dual sub-picosecond and sub-nanosecond laser system

Xinglong Xie (谢兴龙), Fengqiao Liu (刘凤翘), Jingxin Yang (杨镜新), Xin Yang (杨 鑫), Meirong Li (李美荣), Zhiling Xue (薛之玲), Qi Gao (高 奇), Fuyi Guan (管富义), Weiqing Zhang (张伟清), Guanlong Huang (黄关龙), Yifei Zhuang (庄亦飞), Aimei Han (韩爱妹), and Zunqi Lin (林尊琪)

National Laboratory on High Power Laser and Physics, Shanghai Institute of Optics and Fine Mechanics, The Chinese Academy of Sciences, Shanghai 201800

Received March 21, 2003

A high power laser system delivering a 20-TW, 0.5 – 0.8 ps ultra-short laser pulse and a 20-J, 500-ps long pulse simultaneously in one shot is completed. This two-beam laser operates at the wavelength of 1053 nm and uses Nd doped glass as the gain media of the main amplification chain. The chirped-pulse amplification (CPA) technology is used to compress the stretched laser pulse. After compression, the ultra-short laser pulse is measured: energy above 16.0 J, S/N contrast ratio $\sim 10^5 : 1$, filling factor $\sim$>52.7%. Another long pulse beam is a non-compressed chirped laser pulse, which is measured: energy $\sim$ 20 J, pulse duration 500 ps. The two beams are directed onto the target surface at an angle of 15°.

OCIS codes: 140.3280, 190.4970.

In recent years, high power ultrafast lasers are of great interests in the fields of biochemistry, fast ignition of inertial confined fusion (ICF) as well as laser-matter interactions[1−3]. One of the methods to ensure a short laser pulse with even more higher peak power is to use the regenerative and Nd glass amplifiers based chirped-pulse amplification (CPA) technology in which an ultrafast laser pulse is stretched, amplified at first and recompressed into the original temporal width at last[4−7]. Up to now, several laboratories have reported experimental results from several TW to about 1-PW ultrafast laser systems[8−10]. Some of these lasers use all Ti:S crystal to amplify the laser pulse while the others use Ti:S crystal and Nd:glass hybrid resume. In the study of fast ignition of ICF, theoretical and experimental results show that the effective laser facility has not only the high peak power but also the high laser energy. Since the Nd:glass amplifier can support a very large diameter laser beam, Ti:S crystal and Nd:glass hybrid resume is almost used in all high energy ultrafast laser systems. This year, we have established a sub-picosecond and sub-nanosecond Ti:S crystal and Nd:glass hybrid laser system as the platform in study of the PW laser technology as well as some experiments related to laser mater interactions. The laser has two beams whose sub-picosecond beam can deliver a 20 TW peak power laser pulse, temporal width of 0.5 – 0.8 ps, while the other one outputs the long duration laser pulses with pulse width approximately 500 ps, single pulse energy $\sim$ 20 J. Both beams operate at the wavelength of 1053 nm and are directed onto the target surface at an angle of 15°. In this paper the laser system is introduced and some other related characteristics are discussed.

Figures 1 and 2 show the layout of the laser system. It begins with a Kerr-lens mode-locked Ti:sapphire oscillator that outputs a 1053-nm, ~100 fs, 76-MHz, 300-mW (~4 nJ) pulse strain. After a 4-pass stretcher which consists of a single 1800-line/mm grating, a 940-mm focal length aspheric lens, a 15-cm-long, 2.54-cm-wide high reflectance mirror placed at the focal plane of the lens, and a gold-coated retroreflector, the laser pulses are stretched up to 1.0 ns with the total bandwidth of 10 nm.

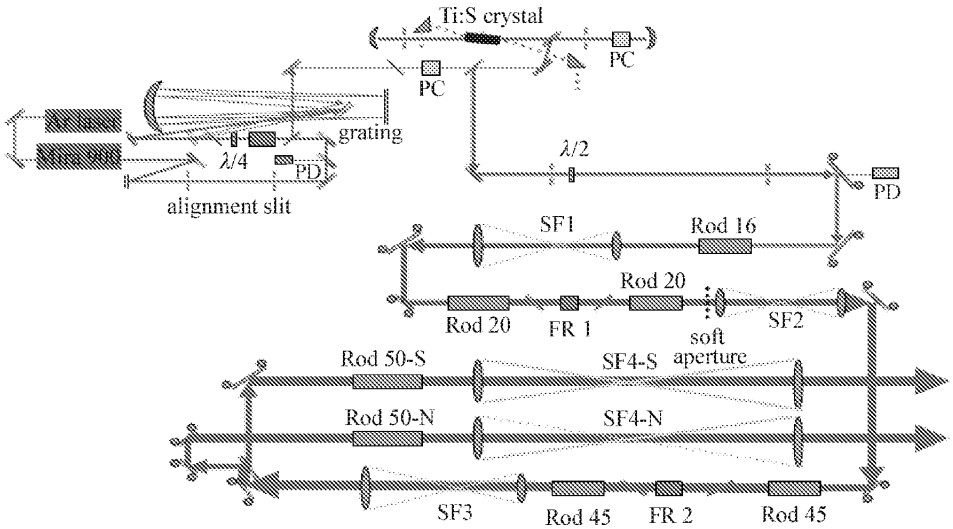

Fig. 1. Schematic view of front-end and main laser bay of dual pulse laser system.

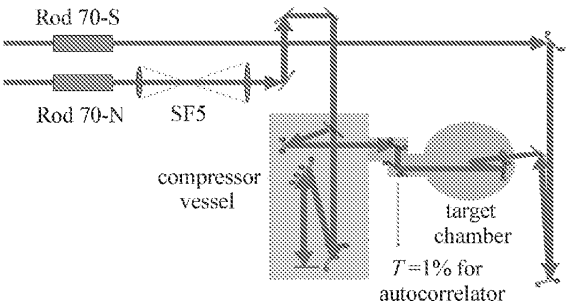

Fig. 2. The target area of dual pulse laser system.

After the stretcher the laser pulse strain is injected into the Ti:sapphire regenerative amplifier. The cavity length of the Ti:sapphire regenerative amplifier is 2.0 m, radii of two cavity mirrors are both 3.0 m, length of Ti:S crystal is 17 mm, Ti doped concentration is 0.15 wt.-%, and it is two-end pumped by a 2ω Nd:YAG laser (Continuum, Surelite-I). The pump pulse energy has been measured to be 75 mJ at one end and 69 mJ at another. Immediately following the pump, single-pass gain is 1.3 (the stimulated cross section $\sigma_e = 2.3 \times 10^{-20}$ cm^2 at 1053 nm). The net gain reaches 10^6 which boosts the laser pulse energy to 1.0 mJ at 10-Hz repetition, and pulse width narrows to 800 ps. Output stability versus round trip number has been studied by assuming that the intracavity beam is a uniform transverse distribution (TEM_{00}), then we use[11,12]

$$J_{\text{out}}^{(p)} = J_{\text{sat}} \ln\{1 + \exp(J_{\text{sto}}^{(p)}/J_{\text{sat}}) \cdot [\exp(J_{\text{in}}^{(p)}/J_{\text{sat}}) - 1]\}, \quad (1)$$

where p is the round-trip number, $J_{\text{in}}^{(p)}$ and $J_{\text{out}}^{(p)}$ are the input and output energy density respectively. Calculations show that there is an optimum round-trip number p with the given input pulse energy. Figure 3 demonstrates that the regenerative amplifier reaches the maximum stability at $p \sim 55$. the measured pulse-to-pulse fluctuations of the regenerative amplifier is $\sim \pm 10\%$.

Further amplification occurs in Nd:doped phosphate-glass ($\sigma_e = 3.5 \times 10^{-20}$ cm^2) rod amplifiers. At first, the chirped laser pulse from the regenerative amplifier passes through one $\phi 16 \times 350$ mm^2 (total gain ~ 50) and two $\phi 20 \times 350$ mm^2 (total gain ~ 900) Nd glass amplifiers,

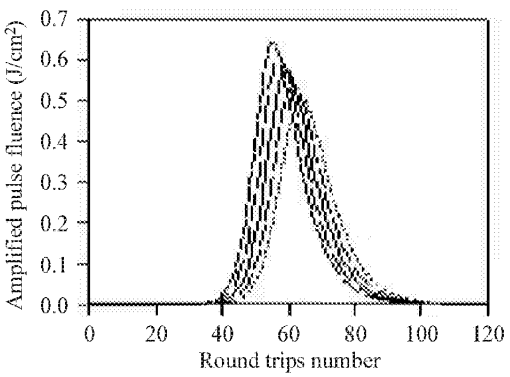

Fig. 3. Output fluence versus number of round-trips.

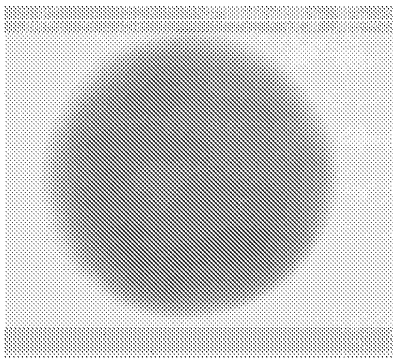

Fig. 4. The burning spot by a laser pulse on the photosensitive paper with the beam diameter 90 mm.

a PC chopper with the transmittance of 0.4, a spatial filter (SF1) with the transmittance of 0.7, and a serrated aperture $\phi 5.4$ mm passes energy approximately 30% that serves as the object plane for the relay image system and reproduces a beam following the second spatial filter (SF2) with a super gaussian profile. Then the laser pulse is directed into two $\phi 40 \times 350$ mm^2 rod amplifiers and a Farady rotator is put between them to eliminate the retroreflecting laser. After the third successive spatial filter (SF3), laser pulse energy is boosted to 5.0 J.

Then the laser beam is split into two parts: ultra-short beam and long pulse beam. The ultra-short one passes through a $\phi 50 \times 350$ mm^2 rod amplifier, a spatial filter (SF4-N), a $\phi 70 \times 350$ mm^2 rod amplifier and the last expanding spatial filter (SF5), the laser pulse energy reaches $\sim$ 20 J, beam diameter is 90 mm, the filling factor $> 50\%$ (shown in Figs. 4 and 5) and spectrum width ~ 3.5 nm (shown in Fig. 6). While the long pulse beam just without the expanding spatial filter, the pulse energy measured is 20 J and beam diameter is 65 mm. After the temporal delay path, it is focused into the target chamber by a non-spherical lens.

In the design of the grating pair compressor, group velocity dispersion (GVD) compensation includes two aspects: second- and third-order GVD which are generated by pulse stretcher, second- and third-order GVD which are generated by preamplifiers and main power amplifiers. GVD calculation of the stretcher is 8.03×10^{-23} s^2. Total length of the amplification chain is 6.0 m, the GVD calculation is 5.0×10^{-26} s^2.

The compressor is a two-pass gold-coated grating pair. Grating parameters are: $390 \times 190 \times 60$ mm^3 in size, 1700-line/mm, center wavelength 1053 nm, incident angle 67.5°, reflectence $> 92\%$. Distance between the center of two gratings is 1127.24 mm. The estimated power density on the gratings is $10^{11} - 10^{12}$ W/cm^2. The entire assembly is housed in a vacuum vessel which is 3 m long and 1 m in diameter, and routinely pumped to a base pressure 10^{-3} Pa. Compressed laser pulse is measured by a single shot autocorrelator. The minimum temporal width is approximately 550 fs, laser pulse energy is estimated to be 16.0 J. Figure 7 shows the autocorrelator trace of the compressed laser pulse. The target chamber is a cylinder design with fourteen detection windows. It is connected with the compressor vacuum vessel by a vacuum tube. A gate valve is set in the tube to isolate both chambers. Focusing of the ultra-short beam is accomplished with an off-axis parabolic mirror (f=300 mm).

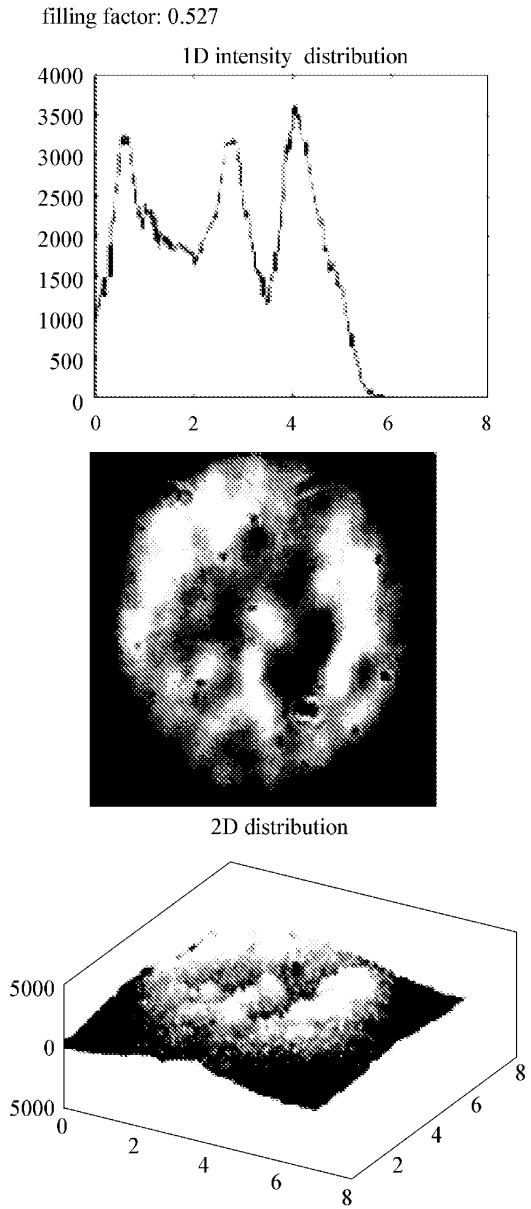

Fig. 5. Near-field measurement of laser pulse by a CCD camera.

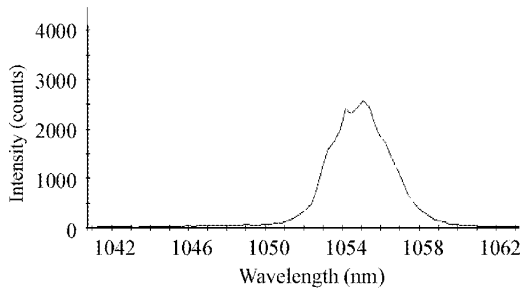

Fig. 6. Measured spectrum width of ultra-short laser pulse at the peak power 20 TW.

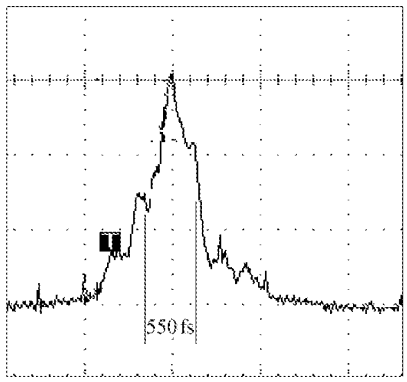

Fig. 7. Measured temporal width of ultra-short laser pulse at the peak power 20 TW.

The long pulse beam is focused by a non-spherical lens and goes to the target at 15° from that of the ultra-short one.

To date, the focal spot size of the laser system is about 30 μm in diameter measured by a CCD far-field camera. Focused by an off-axis parabolic mirror, the power density on target surface is estimated to be 2×10^{18} W/cm^2. In a neutron experiment, a C_8D_8 plate target is placed on the focal spot, maximum neutron yield reaches 2.4×10^4 for one laser shot.

This work was supported by the National 863-804 (former 416)-2 Hi-Tech Program of China. X. Xie's e-mail address is xiexl329@mail.shcnc.ac.cn.

References

1. J. L. A. Chilla and O. E. Martinez, Opt. Lett. **16,** 39 (1991).
2. B. Broers, L. D. Noordan, and H. B. van Linden van den Heuvell, Phys. Rev. A **46,** 2749 (1992).
3. A. M. Weiner, D. E. Laird, G. P. Wiederrecht, and K. A. Nelson, J. Opt. Soc. Am. B **8,** 1264 (1991).
4. C. Chien, in *Dissertation for the Degree of Doctor of Philosophy* (Department of Electrical Engineering, University of Michigan, 1994).
5. B. C. Stuart, S. Herman, and M. D. Perry, IEEE J. Quantum Electron. **33,** 528 (1995).
6. D. Strickland and G. Mourou, Opt. Commun. **56,** 219 (1985).
7. P. Maine, D. Strickland, P. Bado, M. Pessort, and G. Mourou, IEEE J. Quantum Electron. **24,** 398 (1988).
8. M. D. Perry and G. Mourou, Science **264,** 917 (1994).
9. K. Yamakawa, H. Shiraga, Y. Kato, and C. P. Barty, Opt. Lett. **16,** 238 (1991).
10. C. Rouyer, E. Mazataud, I. Allais, A. Pierre, S. Seznec, C. Sauteret, G. Mourou, and A. Migus, Opt. Lett. **18,** 214 (1993).
11. L. M. Frantz and J. S. Nodvik, J. Appl. Phys. **34,** 2346 (1963).
12. F. P. Strohkendl, D. J. Files, and L. R. Dalton, J. Opt. Soc. Am. B **11,** 742 (1994).